

Article

An Environmentally Adaptive Positioning Method Based on Integration of GPS/DTMB/FM

Li Cong ¹, Haidong Wang ¹, Honglei Qin ^{1,*} and Luqi Liu ²

¹ School of Electronic and Information Engineering, Beihang University, 37 Xueyuan Road, Beijing 100191, China; E-mails: congli_bh@buaa.edu.cn; whdtune@gmail.com; qhlmmm@sina.com

² Didi Chuxing Technology Co., Compound 8, Dongbeiwang Road, Beijing 100000, China; liuluqi667@yeah.net

* Correspondence: qhlmmm@sina.com; Tel.: +86-10-8231-6491

Version October 24, 2018 submitted to Sensors

Abstract: Global Positioning System (GPS) yields good precision and availability in open outdoor environment, whereas its accuracy often suffers serious degradation in complex environment like forests and urban canyons due to occlusion, attenuation and multipath. In order to improve positioning accuracy in such complex environment, a positioning method is designed and tested integrating GPS, Digital Terrestrial Multimedia Broadcast (DTMB) and frequency-modulated (FM) radio signal with an adaptive integration mode selection scheme. Major contributions of this paper lie in two aspects. Firstly, the DTMB transmitter is taken as a pseudo-satellite to assist GPS positioning, and positioning result of FM signal fingerprinting is used to correct location yields of the GPS+DTMB system. Secondly, an adaptive integration mode selection scheme is devised to decide the optimal integration mode of GPS, DTMB and FM positioning according to environmental conditions. Field experiment proves that accuracy of the proposed positioning method outperforms those of GPS-only and GPS+DTMB approach in complex environment.

Keywords: Global Positioning System; Digital Terrestrial Multimedia Broadcast; Frequency Modulation; Environmentally Adaptive; Fuzzy Inference System; Extended Kalman Filter

1. Introduction

After decades of development, Global Positioning System (GPS) has become the dominant positioning approach in outdoor environment for its high precision, globalization and real-time response. Advances in technology have facilitated the application of smartphones with cheap GPS receivers, providing users with access to location service in common outdoor environment. However, GPS signal may be confronted with attenuation, occlusion and multipath in scenarios like forests and urban canyons, which often leads to serious deterioration of positioning accuracy, or even failure in positioning. In order to tackle the positioning problem in such complex environment, various positioning techniques have emerged using ultra-wideband (UWB) [1,2], frequency-modulated (FM) radio [3–8], digital television (DTV) [9–12], radio-frequency identification (RFID) [13], WiFi [14–19] and other types of signal. UWB positioning systems locate users using trilateration algorithm with the help of pre-deployed UWB transmitters. High accuracy it may achieve, environment setup costs a lot. RFID-based positioning systems determine users' locations when they are in the vicinities of pre-deployed RFID tags. Effective read distance of RFID tag is usually limited, so it would take both time and labor to deploy large number of tags for the purpose of positioning in vast areas. WiFi positioning, as a popular technique in indoor positioning, is not suitable for outdoor scenarios since it requires good WiFi coverage. As for signal with lower frequency like DTV and FM signal, mature infrastructure and strong propagation ability make them good choices for positioning in areas short

33 of GPS signal. Thus DTV and FM signal are employed in this paper to assist GPS signal to achieve
34 positioning in complex environment with GPS failure.

35 Digital Terrestrial Multimedia Broadcasting (DTMB) is the standard for digital television
36 broadcasting systems in China. Broadcasted by fixed ground stations, DTMB signal excels GPS signal
37 in power by more than 30 dB. Penetration and propagation ability of DTMB signal is stronger than that
38 of GPS signal thanks to its low frequency of 470–860 MHz. Reference time used by DTMB transmitters
39 is strictly synchronized with GPS time. What's more, DTMB signal is structured periodically, with
40 pseudo-random code provided for temporal protection and time synchronization. Based on these
41 characteristics, it's possible for us to use DTMB signal with the trilateration method to locate users
42 when multiple DTMB transmitter is broadcasting. When the number of DTMB transmitters is too small
43 to meet basic positioning requirement, it can also be used as pseudo-satellites to aid GPS positioning.

44 Frequency-modulated (FM) radio broadcasting has long been widely used. Its low frequency,
45 around 100 MHz, makes it much easier to propagate in forests, urban canyon and indoor scenarios
46 than other common signals like GPS, WiFi and DTMB signal. The propagation model approach and
47 the fingerprinting approach are usually employed in FM-based positioning systems. The propagation
48 model method deduce user locations by analyzing signal characteristics measured by the user with
49 prebuilt radio propagation model. The fingerprinting method [20–22] is based on similarity of signal
50 characteristics among locations, whereas the signal characteristics are referred to as "fingerprints" at
51 corresponding locations. Fingerprint positioning is generally divided into two stages: the offline and
52 the online stage. At the offline stage, site survey is conducted to collect fingerprint data at reference
53 points (RPs) and create fingerprint database. At the online stage, fingerprint data at test points (TPs)
54 are compared with the database using feature matching methods to estimate users' positions.

55 The principle of DTMB positioning in our method is similiar to that of GPS, thus it's not difficult
56 for us to aid GPS with DTMB. However, line-of-sight (LOS) propagation of GPS/DTMB signal is
57 required for good precision. On the other hand, FM fingerprint positioning systems can work in
58 environment with little LOS signal, despite the positioning accuracy is not so competitive as that
59 of GPS. What's more, accuracy of FM fingerprint positioning can be improved if GPS is used to
60 constrain the range of RPs. Therefore, we integrate GPS, DTMB and FM signal and adaptively select
61 the integration mode according to environmental conditions to minimize positioning error.

62 In this paper, an outdoor positioning system combining GPS, DTMB and FM signals is designed to
63 tackle the positioning problem in complex outdoor environment. The proposed system can adaptively
64 select the appropriate integration mode of the three signals by analyzing environmental characteristics,
65 and then fuse information from part or all of the three signals with an Extended kalman Filter (EKF) to
66 yield the optimal positioning result.

67 The rest of the paper is organized as follows: section 2 introduces the overall system architecture,
68 section 3 describes the details, section 4 is the design of the mode selection scheme, section 5 explains
69 design of the sensor fusion filter, in section 6 experiments and result analysis are provided, and finally
70 in section 7 conclusions and future works are summarized.

71 2. System Architecture

72 The integrated positioning system designed in this paper consists of three parts: hardware
73 equipment, software processing and local storage, as shown in Figure 1. Hardware equipment includes
74 GPS antenna and receiver, DTMB antenna and receiver, as well as FM antenna and receiver. With the
75 hardware equipment we can receive and extract raw information from the signals. Software processing
76 is composed of three stages: preprocessing, adaptive integration mode selection and information
77 fusion with an EKF. At the preprocessing stage, GPS is employed to assist DTMB and FM according
78 to environmental conditions and input for the integration mode selection stage is computed. At the
79 mode selection stage, a fuzzy inference system is utilized to select the appropriate integration mode
80 of GPS, DTMB and FM signals based on several environmental indicators. At the information fusion
81 stage, information from the three signals are fused with EKF to estimate user locations based on mode

selection result. Information needed by software processing, such as DTMB pseudo-noise sequence and FM fingerprint database, is managed by local storage.

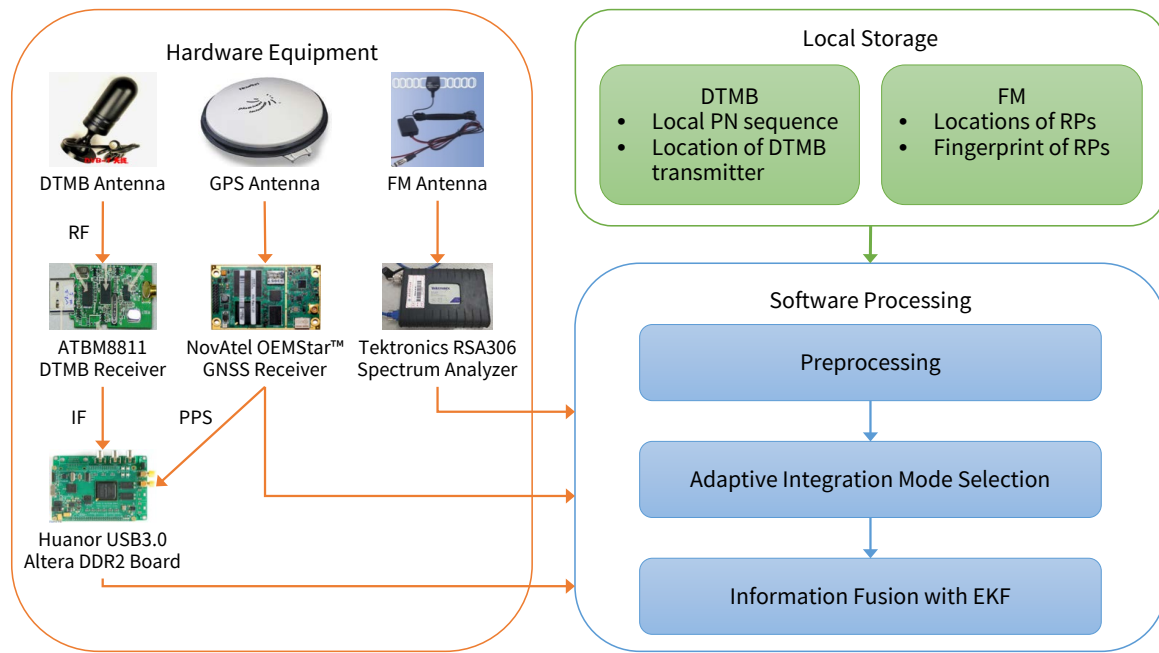


Figure 1. Overall architecture of the proposed system

3. Preprocessing

Software processing is made up of preprocessing, adaptive mode selection and EKF filtering. Flow chart of the preprocessing part is shown as illustrated in Figure 2. First, check whether GPS positioning result is available by the number of visible satellites. If it is, calculate geometric dilution of precision (GDOP) of GPS positioning and check whether we can use GPS to correction clock error of DTMB. Then if the correction is permitted, it is conducted and GDOP of GPS+DTMB positioning is calculated as input variable for mode selection part. If the number of visible satellites is too few for us to get reliable GPS positioning results, FM fingerprint positioning would be performed. And if GPS positioning had been performed before, we can exploit previous GPS positioning results to attain an estimation of current user location, and use it to remove FM RPs too far from it for better accuracy. Errors of DTMB-only or FM-only positioning are often larger than those of GPS only, thus it's necessary to perform DTMB clock error correction and FM RP selection with GPS data for location accuracy improvement. GDOP of GPS alone, GDOP of GPS+DTMB, and RP number within constraint range, are needed in the integration mode selection stage.

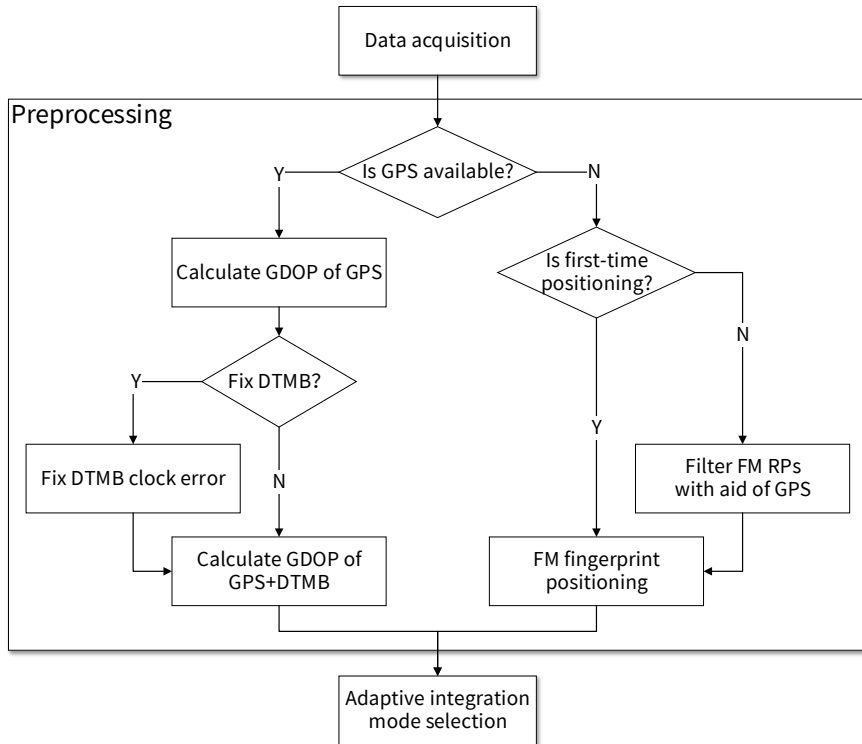


Figure 2. Flow chart of preprocessing

98 3.1. DTMB Clock Error Correction

When GDOP of GPS is no greater than a certain threshold, it can be considered that positioning requirement is satisfied and we can use GPS positioning results to correct clock error of the DTMB receiver.

102 Equation 1 shows the relationship between satellite positions and user location in GPS positioning.

$$\rho_s^i = \sqrt{(x^i - x)^2 + (y^i - y)^2 + (z^i - z)^2} + c \cdot \Delta t_u \quad (i = 1, 2, \dots, N) \quad (1)$$

$$\rho_d = \sqrt{(x^d - x)^2 + (y^d - y)^2 + (z^d - z)^2} + c \cdot \Delta t_d \quad (2)$$

103 It reveals the position relationship between user and the i -th GPS satellite, where ρ_s^i is the pseudorange
 104 of the satellite, $[x^i, y^i, z^i]$ is the position of the satellite, $[x, y, z]$ is user's location, c is the speed of light,
 105 Δt_u is the clock error of GPS receiver and N is the number of available GPS satellites. Equation 2
 106 shows the position relationship between user and DTMB transmitter, where ρ_d is the pseudorange
 107 between user and the transmitter, $[x^d, y^d, z^d]$ is the position of the transmitter and Δt_d is the clock error
 108 of DTMB receiver. When there are at least 4 GPS satellites available, we can obtain user position with
 109 Equation 1, after which Δt_d , clock error of DTMB, can be attained with Equation 2. In this way clock
 110 error correction for DTMB is performed.

111 3.2. FM RP Selection

If GDOP of GPS is small enough, GPS system can also be employed to improve positioning accuracy of FM fingerprinting. It's the basic assumption for fingerprint localization that spacial proximity is proportional to similarity of signal characteristics. However, this assumption is not always true in actual conditions. There is possibility that RP with the highest similarity in signal characteristics is far from the TP, whereas RPs in the vicinity of the TP demonstrates low similarity with it, as shown in Figure 3a. Therefore, GPS positioning result is utilized to filter out RPs too far from current TP to reduce such cases. When GPS positioning condition is good enough, we can take the GPS positioning

result as the tentative position of TP, and draw a circle on the ground plane with some radius, as illustrated in Figure 3b. To restrict the upper bound of positioning error, only RPs within this circle can be selected for computation of fingerprinting result. On the other hand, when GPS positioning result is not reliable, we can deduce user's position with previous reliable GPS positioning results and increase the radius of the circle. This is usually effective when GDOP of GPS has just begun to deteriorate.

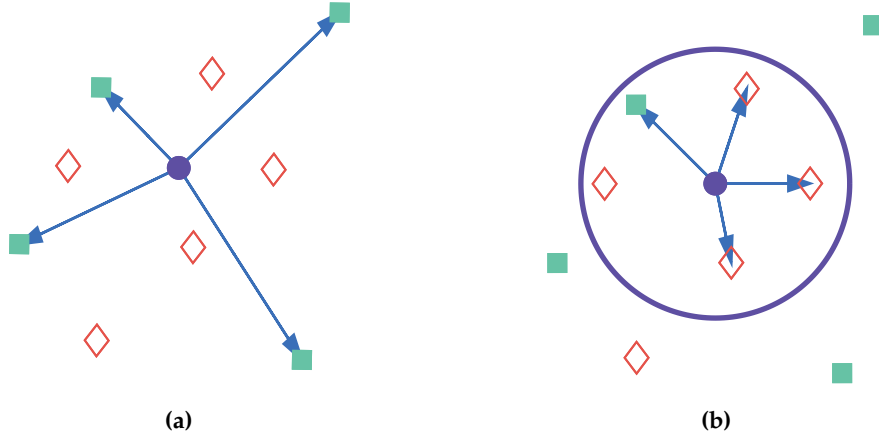


Figure 3. Demonstration of RP constraint. (a) RP selection result without GPS constraint. (b) RP selection result with GPS constraint. In both figures,, the purple circles are TPs. In subfigure (a), cyan rectangles connected with TP by arrows are selected RPs and red diamonds are RPs not selected for computation of TP's position. In subfigure (b), points connected with TP by arrows are selected RPs, the purple circle shows the constraint range.

124 4. Adaptive Integration Mode Selection

125 There are various factors indicating environment conditions, such as GDOP of GPS and
 126 GPS+DTMB, as well as the number of RPs within constraint range for FM. It's not easy to find a
 127 specific formula describing the relationship between integration mode and these factors. Thus, we
 128 adopt the fuzzy inference approach to combine these factors and find the optimal integration mode of
 129 GPS, DTMB and FM signals.

130 Fuzzy inference systems are predicated upon the fuzzy set theory. In set theory, the relationship
 131 between an element and a set is crisp, either belonging to or not belonging to. However, the relationship
 132 between an element and a fuzzy set is described by membership ranged from 0 to 1. The crisp
 133 inputs would be fuzzified into membership to fuzzy sets, but the final outputs are crisp values after
 134 defuzzification.

The inputs of our fuzzy inference system are GDOP of GPS, GDOP of GPS+DTMB, and number of FM RPs within constraint range. And the output is the integration mode: GPS only, GPS+DTMB, and GPS+DTMB+FM. First membership functions, in our system trigonometric membership functions are utilized, are used to fuzzify the inputs and convert them into membership. Then we need to create fuzzy rules to connect inputs and outputs. The fuzzy rules in our system can be described as below:

$$R^i : \quad \text{IF } x_1 \subset X_1^a \text{ AND } x_2 \subset X_2^b \text{ AND } x_3 \subset X_3^c \\ \text{THEN } y \subset Y^d, \quad a, c = 1, 2; b, d = 1, 2, 3; i = 1, 2, \dots, n \quad (3)$$

135 where R^i denotes the i -th rule, x_1, x_2 , and x_3 are the fuzzified inputs, X_1^p, X_2^q , and X_3^r are the fuzzy sets
 136 for inputs, y is the output before defuzzification, Y^d is the fuzzy set for output.

137 There are two fuzzy sets for both of input x_1 and x_3 for description of small and large values
 138 of them, correspondingly X_1^S, X_1^L, X_2^S and X_2^L . For input x_2 , three fuzzy sets are used, X_2^S, X_2^M and
 139 X_2^L , for description. The three integration mode are denoted by Y^A, Y^B and Y^C , as shown in Table 1.

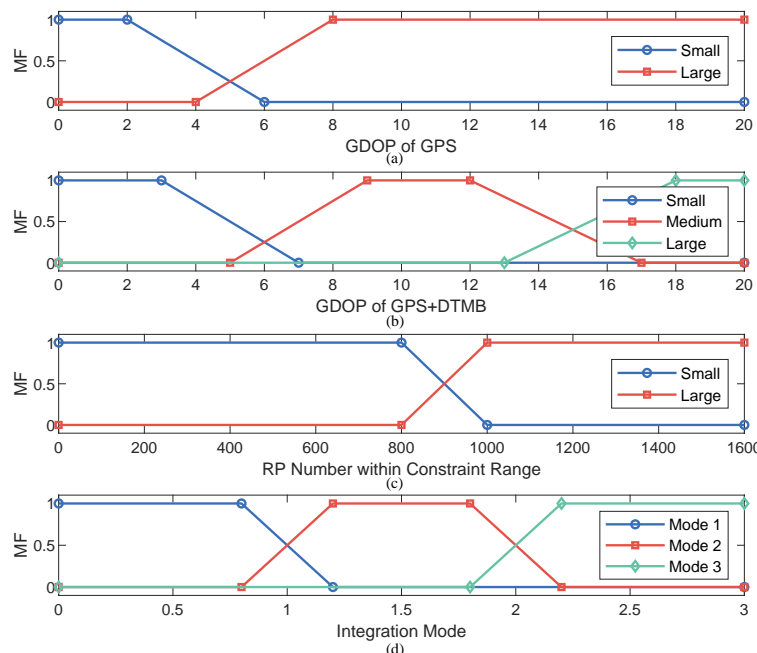
¹⁴⁰ Membership functions for inputs and outputs of the fuzzy inference system is shown as Figure 4. In
¹⁴¹ this way all fuzzy rules are demonstrated as Table 2.

Table 1. Symbols for Integration Modes

Integration Mode	Symbol
GPS only	Y^A
GPS+DTMB	Y^B
GPS+DTMB+FM	Y^C

Table 2. Fuzzy Rules in Our System

x_1	x_2	X_2^S	X_2^M	X_2^L	X_3^S	X_3^M	X_3^L
x_3	X_2^S	X_3^S	X_3^M	X_3^L	X_2^S	X_2^M	X_2^L
		Y^A	Y^A	Y^A	Y^A	Y^A	Y^A
		Y^A	Y^A	Y^B	Y^C	Y^C	Y^C

**Figure 4.** Membership functions in our fuzzy inference system. (a) Membership function for GDOP of GPS. (b) Membership function for GDOP of GPS+DTMB. (c) Membership function for RP number within constraint range. (d) Membership function for system output (integration mode).

¹⁴² 5. Design of Integration Filter

¹⁴³ In this paper, EKF is utilized for fusion of information from multiple sources. The design of state
¹⁴⁴ model and observation model in our EKF filter is explained in detail as below.

145 5.1. State Model

System state in our filter is a vector of 11 dimensions, including position, velocity, acceleration, clock error and frequency error of user's receiver, as illustrated in Equation 4.

$$\mathbf{x} = [x, \dot{x}, \ddot{x}, y, \dot{y}, \ddot{y}, z, \dot{z}, \ddot{z}, \delta t, \delta f]^T \quad (4)$$

146 where $[x, y, z]$ is receiver coordinate in earth-centered earth-fixed (ECEF) coordinate system, $[\dot{x}, \dot{y}, \dot{z}]$ is
147 receiver velocity in ECEF coordinate system, $[\ddot{x}, \ddot{y}, \ddot{z}]$ is receiver acceleration in ECEF coordinate system,
148 δt is receiver clock error, and δf is receiver frequency error. In the integrated system, acquisition of
149 DTMB signal is triggered by GPS pulses-per-second signal. And DTMB clkok error would be corrected
150 with aid of GPS when the latter is ready for use. Therefore, it can be deemed that clock time of the GPS
151 receiver and that of DTMB receiver is approximately synchronized, and the two receivers also share
152 the same clkok erro and frequency error.

153 By referring to established model, we designed the discrete state model of the filter as Equation 5:

$$\mathbf{x}_{k+1} = \Phi_k \cdot \mathbf{x}_k + \boldsymbol{\omega}_k = \begin{bmatrix} \mathbf{M} & 0 & 0 & 0 \\ 0 & \mathbf{M} & 0 & 0 \\ 0 & 0 & \mathbf{M} & 0 \\ 0 & 0 & 0 & \mathbf{A}_c \end{bmatrix} \mathbf{x}_k + \boldsymbol{\omega}_k \quad (5)$$

where $\mathbf{M} = \begin{bmatrix} 1 & T & T^2/2 \\ 0 & 1 & T \\ 0 & 0 & 1 \end{bmatrix}$, $\mathbf{A}_c = \begin{bmatrix} 1 & T \\ 0 & 1 \end{bmatrix}$, T is the differential interval, and $\boldsymbol{\omega}_k$ is the process noise
vector. The covariance matrix of $\boldsymbol{\omega}_k$, \mathbf{Q} , is:

$$\mathbf{Q} = \begin{bmatrix} \mathbf{Q}_p & \mathbf{0} \\ \mathbf{0} & \mathbf{Q}_c \end{bmatrix} \quad (6)$$

In Equation 6, $\mathbf{Q}_p = [\mathbf{Q}_x, \mathbf{Q}_y, \mathbf{Q}_z]^T$, and $\mathbf{Q}_k (k = x, y, z)$ is the covariance matrix of vector $[k, \dot{k}, \ddot{k}]^T (k = x, y, z)$. $\mathbf{Q}_k (k = x, y, z)$ can be obtained as Equation 7:

$$\mathbf{Q}_k = S_{a,k} \begin{bmatrix} T^5/20 & T^4/8 & T^3/6 \\ T^4/8 & T^3/3 & T^2/2 \\ T^3/6 & T^2/2 & T \end{bmatrix}, \quad (k = x, y, z) \quad (7)$$

where $S_{a,k}$ is the power spectral density of receiver acceleration with respect to k axis. On the other hand, \mathbf{Q}_c in Equation 6 is the covariance matrix of the vector $[\delta t, \delta f]^T$ and it can be attained as Equation 8:

$$\mathbf{Q}_c = \begin{bmatrix} S_t T + S_f T^3/3 & S_f T^2/2 \\ S_f T^2/2 & S_f T \end{bmatrix} \quad (8)$$

154 where S_t and S_f are the noise power spectral density of clock error and frequency error.

155 5.2. Observation Model

156 There are three types of observations in our filter: pseudorange obtained from GPS and DTMB,
157 pseudorange rate from GPS, and position coordinate from FM.

158 5.2.1. Pseudorange as Observation

The pseudorange of the i -th satellite, ρ^i , can be expressed as below:

$$\rho^i = h_s(\mathbf{x}) = [(x_s^i - x)^2 + (y_s^i - y)^2 + (z_s^i - z)^2]^{1/2} + \Delta t + \varepsilon_\rho^i, \quad (i = 1, 2, \dots, N) \quad (9)$$

where N is the total number of satellites, $[x_s^i, y_s^i, z_s^i]^T$ is satellite position in ECEF coordinate system calculated from GPS ephemeris and ε_ρ^i the is measurement noise of pseudorange. The partial derivatives of $h_s(\mathbf{x})$ are as follows:

$$\begin{aligned}\frac{\partial h_s}{\partial x} &= -\frac{x_s^i - \hat{x}}{[(x_s^i - \hat{x})^2 + (y_s^i - \hat{y})^2 + (z_s^i - \hat{z})^2]^{1/2}} \\ &= \frac{\hat{x} - x_s^i}{r^i} = e_1^i\end{aligned}\quad (10)$$

$$\frac{\partial h_s}{\partial y} = \frac{\hat{y} - y_s^i}{r^i} = e_2^i \quad (11)$$

$$\frac{\partial h_s}{\partial z} = \frac{\hat{z} - z_s^i}{r^i} = e_3^i \quad (12)$$

In Equation 10, 11 and 12, $e_j^i (i = 1, 2, \dots, N; j = 1, 2, 3)$ denote the partial derivative $\partial h_s / \partial k (k = x, y, z)$ and $r^i (i = 1, 2, \dots, N)$ is the distance between user and the i -th satellite. Thus, assuming the number of visible satellites is m , the Jacobian matrix of $h_s(\mathbf{x})$ is as Equation 13:

$$\mathbf{H}_{\rho,s} = \begin{bmatrix} e_{11} & 0 & 0 & e_{12} & 0 & 0 & e_{13} & 0 & 0 & 1 & 0 \\ e_{21} & 0 & 0 & e_{22} & 0 & 0 & e_{23} & 0 & 0 & 1 & 0 \\ \vdots & \vdots \\ e_{m1} & 0 & 0 & e_{m2} & 0 & 0 & e_{m3} & 0 & 0 & 1 & 0 \end{bmatrix} \quad (13)$$

Similarly, pseudorange of DTMB is shown as below:

$$\rho_d = h_d(\mathbf{x}) = [(x_d - x)^2 + (y_d - y)^2 + (z_d - z)^2]^{1/2} + \Delta t + \varepsilon_\rho \quad (14)$$

where $[x_d, y_d, z_d]^T$ is the position of DTMB transmitter in ECEF coordinate system and ε_ρ is the measurement noise of DTMB pseudorange. And we can also get a Jacobian matrix for pseudorange:

$$\mathbf{H}_{\rho,d} = \begin{bmatrix} (\hat{x} - x_d)/r & 0 & 0 & (\hat{y} - y_d)/r & 0 & 0 & (\hat{z} - z_d)/r & 0 & 0 & 1 & 0 \end{bmatrix} \quad (15)$$

159 From above we can know observation model is the same for pseudorange of both GPS and DTMB.
160 Therefore the DTMB transmitter is taken as a pseudo satellite in our algorithm and Equation 9 is the
161 uniform observation equation when pseudorange is used as observation.

162 5.2.2. Pseudorange Rate as Observation

From Equation 9 we can get the observation equation when pseudorange rate is employed as observation:

$$\dot{\rho}_s^i = \frac{\partial \rho_s^i}{\partial t} = e_1^i(\dot{x}_s^i - \dot{x}) + e_2^i(\dot{y}_s^i - \dot{y}) + e_3^i(\dot{z}_s^i - \dot{z}) + \Delta f + \varepsilon_{\dot{\rho}}, \quad (i = 1, 2, \dots, N) \quad (16)$$

where $[\dot{x}_s^i, \dot{y}_s^i, \dot{z}_s^i]^T$ is satellite velocity in ECEF coordinate system computed from satellite ephemeris. And the corresponding Jacobian matrix is:

$$\mathbf{H}_{\dot{\rho},s} = \begin{bmatrix} 0 & e_{11} & 0 & 0 & e_{12} & 0 & 0 & e_{13} & 0 & 0 & 1 \\ 0 & e_{21} & 0 & 0 & e_{22} & 0 & 0 & e_{23} & 0 & 0 & 1 \\ \vdots & \vdots \\ 0 & e_{m1} & 0 & 0 & e_{m2} & 0 & 0 & e_{m3} & 0 & 0 & 1 \end{bmatrix} \quad (17)$$

¹⁶³ 5.2.3. Position as Observation

Position information can be obtained from FM fingerprint positioning. When we use FM signal to correct state predictions, position $\mathbf{z}_f = [x_f, y_f, z_f]^T$ from FM fingerprinting is used as observation. The corresponding observation equation is as follows:

$$\mathbf{z}_f = \begin{bmatrix} x_f \\ y_f \\ z_f \end{bmatrix} + \begin{bmatrix} \varepsilon_x \\ \varepsilon_y \\ \varepsilon_z \end{bmatrix} = \mathbf{H}_f \mathbf{x}_k + \boldsymbol{\varepsilon}_f \quad (18)$$

where $\mathbf{H}_f = [\text{diag}[1 \ 1 \ 1] \ \mathbf{0}_{3 \times 8}]_{3 \times 11}$ and $\boldsymbol{\varepsilon}_f$ is the measurement noise of position. The covariance matrix of $\boldsymbol{\varepsilon}_f$ is:

$$\mathbf{R}_f = E[\boldsymbol{\varepsilon}_f \boldsymbol{\varepsilon}_f^T] = \begin{bmatrix} \sigma_{x,f}^2 & & \\ & \sigma_{y,f}^2 & \\ & & \sigma_{z,f}^2 \end{bmatrix} \quad (19)$$

¹⁶⁴ where $\sigma_{x,f}^2$, $\sigma_{y,f}^2$ and $\sigma_{z,f}^2$ are the positioning error variance of FM fingerprinting with respect to x , y
¹⁶⁵ and z direction.

¹⁶⁶ 6. Experiments and Analysis

The proposed algorithm is tested in the campus of Beihang University. The test region, with an area of around $380m \times 380m$, is shown in Figure 5. There are in total 50 points chosen as TP and 282 chosen as RP for data collection. Then Kriging interpolation is applied to our collected RP fingerprints to increase reference point density in a grid style. After interpolation, there are 16,640 RPs in total and the minimum distance between two RPs is 3m. All of GPS, DTMB and FM signals are received and measured at test points, whereas only FM signal is measured at reference points. For GPS, the signal used by us is GPS L1 signal. For DTMB, it's DTMB Channel 14 in Beijing. As for FM radio, 21 channels with strong signal strength in Beijing are selected.

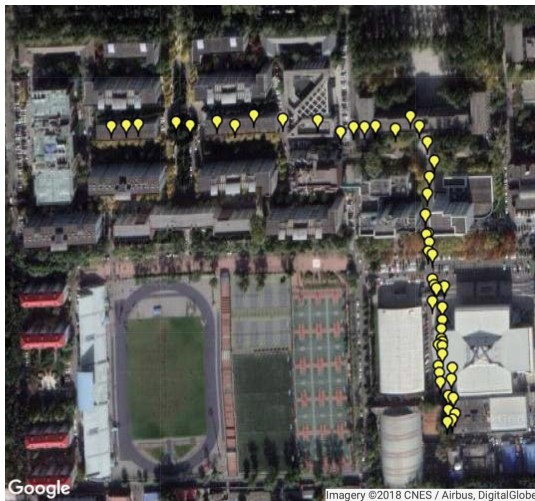


Figure 5. Test area and test points. The yellow markers on the map denote the test points.

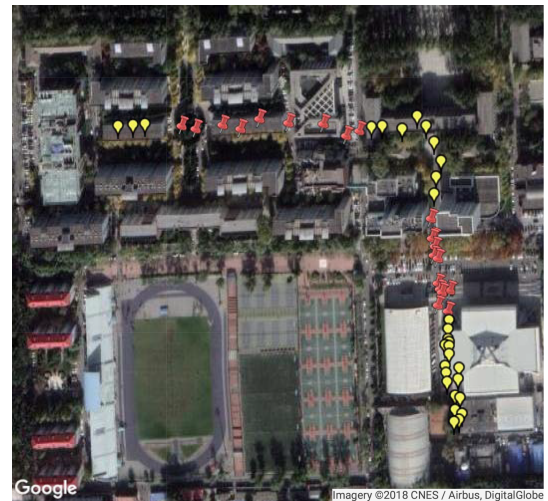


Figure 6. Illustration of points with and without manual satellite loss. The cyan pushpins are points with satellite loss.

¹⁷⁵ Since the availability of GPS satellites in our test area is rather good (no less than 5 satellites
¹⁷⁶ available at each TP), loss of satellite signal is achieved by manual shielding some of the satellites. Two
¹⁷⁷ subareas are chosen as area with satellite loss, where available satellite number is restricted to three.
¹⁷⁸ For simplification of expression, the 50 TPs are numbered from 1 to 50. TPs numbered from 4 to 15 and
¹⁷⁹ from 31 to 46 are test points with satellite loss, as shown in Figure 6. Number of available satellites at

each point before and after manual shielding is shown as Figure 7. The vertical dashed lines in the figures denote the boundaries between areas with and without satellite loss. From Figure 7 we can know that at each point without satellite loss there are at least 5 satellites available. The GDOP of each point under GPS-only and GPS+DTMB mode is illustrated in Figure 8. Here we manually set GDOP to 20 when it exceeds 20 for convenience in figure plotting. Putting Figure 7 and 8 together, it can be seen that there are at least 6 available satellites without satellite loss and GDOP of GPS-only mode is no greater than 5. When the number of available satellites is reduced to 3, GDOP of GPS-only mode spikes to 20. However, once DTMB is introduced to work together with GPS, GDOP stays below that of GPS-only in most of the time, especially in the case of satellite loss. Therefore it can be concluded that DTMB can improve satellite geometric distribution when the availability of GPS satellites is poor.

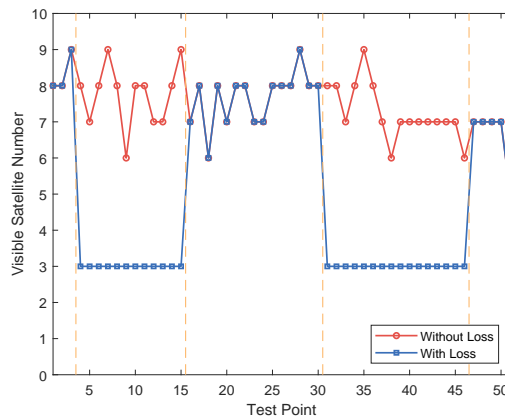


Figure 7. Number of available satellites at each test point

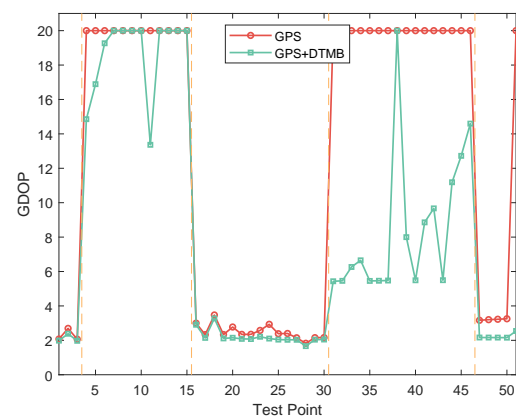


Figure 8. GDOP at each test point

Then the proposed fuzzy inference system is applied to the test data to know the optimal integration mode at each of the test points. The inputs and output of the fuzzy system is shown as Figure 9. The test points are divided into five sections by the four vertical dashed lines. For points indexed 1, 2 and 3 in the first section, GPS-only positioning error stays low with sufficient available satellites, leading to choice of the GPS-only mode. In the second section, the GPS-only mode is no longer chosen because GDOP of GPS-only mode increases due to satellite loss. At this time, GDOP of GPS+DTMB varies with time. When GDOP of GPS+DTMB is relatively small, this mode is preferred. However, if it's too large, FM would be introduced to assist them, which is the GPS+DTMB+FM mode. In the third section, available satellite number become adequate again and GPS-only mode is chosen again. In the fourth section, GDOP of GPS+DTMB is relatively small in most of the time, resulting in the choice of the GPS+DTMB mode. Under some circumstances where GDOP of GPS+DTMB is not small enough and RP number within constraint range is sufficient, the GPS+DTMB+FM mode can yield more precise positioning results. In the last section, GPS-only mode is selected when there is enough available satellites. In other cases where GDOP of GPS is too large, the GPS+DTMB mode is favored as GDOP is limited to a small level with the help of DTMB.

After explanation of the mode selection process, we'd like to compare the positioning error of the proposed method with that of GPS and GPS+DTMB. Positioning error of each test point is shown in Figure 10, from where it's illustrated that overall positioning accuracy of the proposed method outperforms the other two, while the incorporation of DTMB reduces positioning error of GPS. Errors of the three methods in latitude/longitude/altitude direction are also provided as Figure 11, where we can find that the proposed method excels the other two in the three directions in most of the time. Then the true positions of the test points are connected as a virtual trajectory and compared with the trajectories connected by positioning results as Figure 12. It's shown in Figure 12 that plane location error is small with good GPS availability and increases when confronted with satellite loss. At most

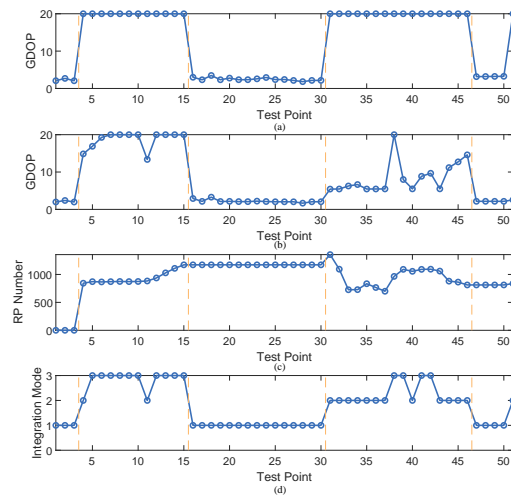


Figure 9. Inputs and output of fuzzy inference system. (a) GDOP of GPS-only mode. (b) GDOP of GPS+DTMB. (c) Number of RPs within constraint range. (d) Integration Mode, also output of the fuzzy system.

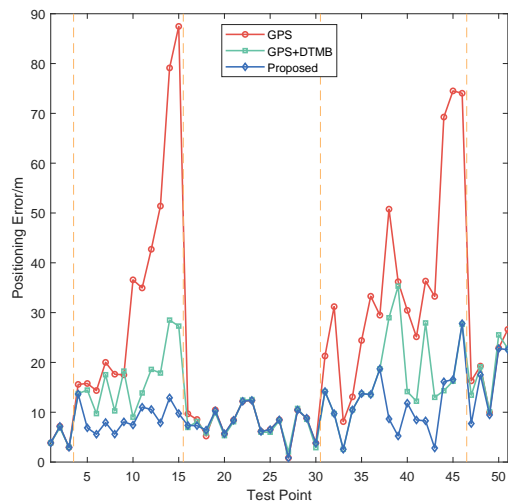


Figure 10. Positioning error at each test point

points, plane location error of the proposed method is smaller than either of GPS-only or GPS+DTMB method, in consistent with results of Figure 11.

For better evaluation of error performance of the proposed method, empirical cumulative distribution functions (CDF) of the three methods are shown in Figure 13. The 1σ , 2σ and 3σ errors are also concluded as Table 3, from where we can know that 3σ error of the proposed method is 21.27% less than that of GPS+DTMB and 68.21% less than that of GPS. From the error distribution data in Figure 13 and Table 3, it can be concluded that positioning error of GPS+DTMB is smaller than that of GPS, and the proposed method can further improve positioning accuracy with the aid of information from GPS, DTMB and FM.

Table 3. Errors of different positioning methods

Positioning Method	1σ Error/m	2σ Error/m	3σ Error/m
GPS	29.49	74.51	87.46
GPS+DTMB	14.46	28.5	35.31
Proposed	10.56	22.57	27.80

7. Conclusion

In this paper, an outdoor positioning method with integration of GPS/DTMB/FM signal and adaptive integration mode selection is proposed and its error performance is tested. On one hand, when faced with shortage of available GPS satellites, DTMB is introduced as information supplement for GPS positioning when faced with satellite shortage, and FM is utilized to cooperate with GPS for positioning accuracy improvement. On the other hand, a fuzzy inference system is designed to determine the most appropriate integration mode of GPS, DTMB and FM signals based on indicators of environment condition. Proof is provided by field test for that the proposed method can make reasonable choices on integration mode according to environment conditions when confronted with shortage of available GPS satellites and yield more precise positioning results than GPS-only and GPS+DTMB method.

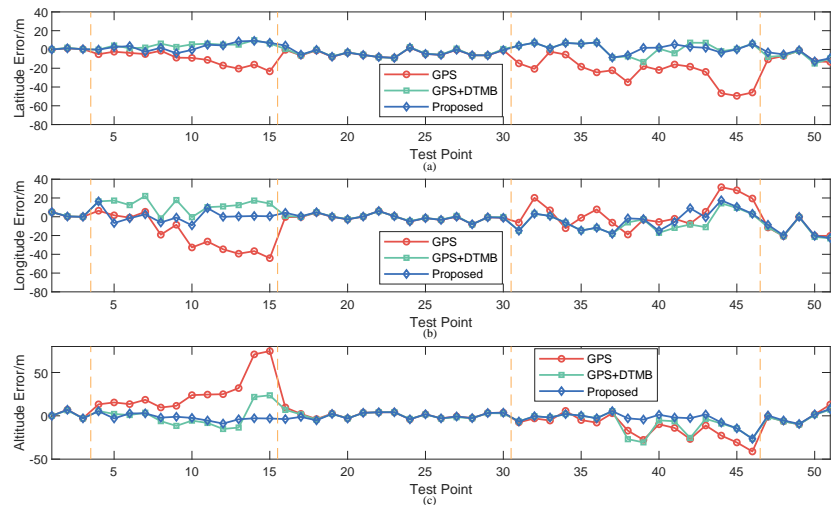


Figure 11. Positioning error of each point in latitude/longitude/altitude direction. (a) Error in latitude direction. (b) Error in longitude direction. (c) Error in altitude direction.

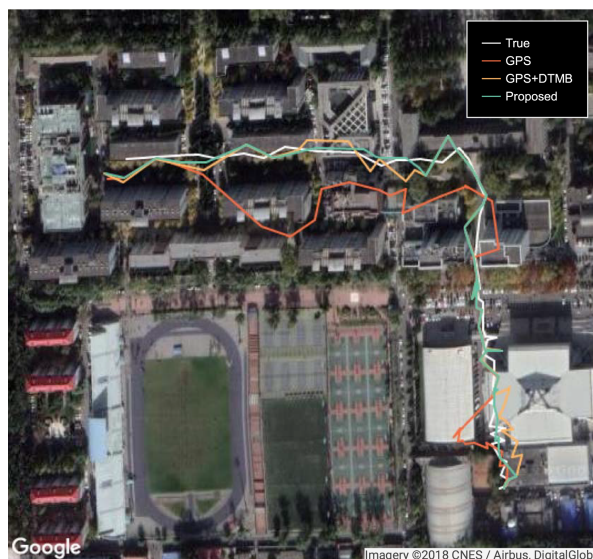


Figure 12. Trajectories generated from true positions and positioning results

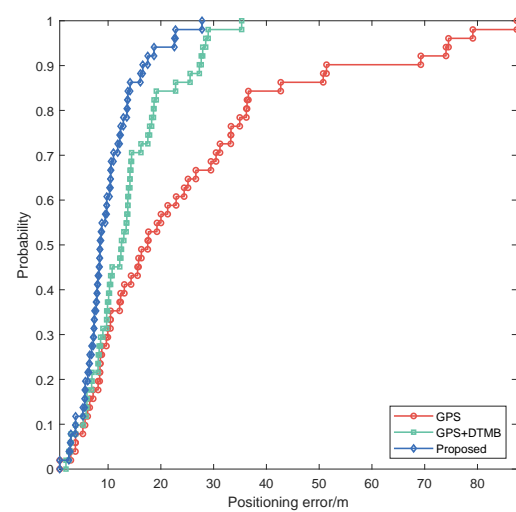


Figure 13. Empirical CDF curves of proposed method, GPS-only method and GPS+DTMB method

Author Contributions: Conceptualization, Li Cong; Data curation, Luqi Liu; Formal analysis, Haidong Wang; Funding acquisition, Honglei Qin; Investigation, Luqi Liu; Methodology, Li Cong; Project administration, Honglei Qin; Resources, Li Cong; Software, Li Cong; Supervision, Li Cong; Validation, Li Cong; Visualization, Haidong Wang; Writing – original draft, Haidong Wang; Writing – review & editing, Li Cong.

Funding: This research is funded by General Armaments Department, People's Liberation Army with grant number 41415060303.

Conflicts of Interest: The authors declare no conflict of interest.

References

1. Tiemann, J.; Schweikowski, F.; Wietfeld, C. Design of an UWB indoor-positioning system for UAV navigation in GNSS-denied environments. 2015 International Conference on Indoor Positioning and Indoor Navigation (IPIN), 2015, pp. 1–7. doi:10.1109/IPIN.2015.7346960.
2. Kolakowski, J.; Consoli, A.; Djaja-Josko, V.; Ayadi, J.; Morrigia, L.; Piazza, F. UWB localization in EIGER indoor/outdoor positioning system. 2015 IEEE 8th International Conference on Intelligent Data Acquisition and Advanced Computing Systems: Technology and Applications (IDAACS), 2015, Vol. 2, pp. 845–849. doi:10.1109/IDAACS.2015.7341422.
3. Chen, Y.; Lymberopoulos, D.; Liu, J.; Priyantha, B. FM-based Indoor Localization. Proceedings of the 10th International Conference on Mobile Systems, Applications, and Services; ACM: New York, NY, USA, 2012; MobiSys '12, pp. 169–182. doi:10.1145/2307636.2307653.
4. Moghtadaiee, V.; Dempster, A.G.; Lim, S. Indoor localization using FM radio signals: A fingerprinting approach. 2011 International Conference on Indoor Positioning and Indoor Navigation, 2011, pp. 1–7. doi:10.1109/IPIN.2011.6071932.
5. Moghtadaiee, V.; Dempster, A.G. Indoor Location Fingerprinting Using FM Radio Signals. *IEEE Transactions on Broadcasting* **2014**, *60*, 336–346. doi:10.1109/TBC.2014.2322771.
6. Andrei, P. Indoor positioning using FM radio signals. PhD thesis, University of Trento, 2011.
7. Popovtsev, A.; Osmani, V.; Mayora, O. Investigation of indoor localization with ambient FM radio stations. 2012 IEEE International Conference on Pervasive Computing and Communications, 2012, pp. 171–179. doi:10.1109/PerCom.2012.6199864.
8. Yoon, S.; Lee, K.; Yun, Y.; Rhee, I. ACMI: FM-Based Indoor Localization via Autonomous Fingerprinting. *IEEE Transactions on Mobile Computing* **2016**, *15*, 1318–1332. doi:10.1109/TMC.2015.2465372.
9. Shang, L.; Menglou, R.; Yunzheng, T.; Long, L.; Ping, Z. A virtual TDOA localization scheme of Chinese DTMB signal in radio monitoring networks. *China Communications* **2015**, *12*, 1–13. doi:10.1109/CC.2015.7366239.
10. Fu, C.; Tian, Z.; Tian, A. Application of the EKF Algorithm in the DTMB Positioning System. Communications, Signal Processing, and Systems; Liang, Q.; Mu, J.; Wang, W.; Zhang, B., Eds.; Springer Singapore: Singapore, 2018; pp. 533–539.
11. Wu, H.; Wang, Q.; Zhao, Y.; Ma, X.; Yang, M.; Liu, B.; Tang, R.; Xu, X. Indoor localization using FM radio and DTMB signals. *Radio Science* **2016**, *51*, 1030–1037. doi:10.1002/2016RS006060.
12. Wu, X.; Zhang, C.; Sohn, S. Ranging and Positioning Algorithm Based on DTMB System. 2018 IEEE International Symposium on Broadband Multimedia Systems and Broadcasting (BMSB), 2018, pp. 1–5. doi:10.1109/BMSB.2018.8436789.
13. Xu, H.; Ding, Y.; Li, P.; Wang, R.; Li, Y. An RFID Indoor Positioning Algorithm Based on Bayesian Probability and K-Nearest Neighbor. *Sensors* **2017**, *17*, 1806. doi:10.3390/s17081806.
14. He, S.; Chan, S.G. Wi-Fi Fingerprint-Based Indoor Positioning: Recent Advances and Comparisons. *IEEE Communications Surveys Tutorials* **2016**, *18*, 466–490. doi:10.1109/COMST.2015.2464084.
15. Wang, C.L.; Chiou, Y.S. An Adaptive Positioning Scheme Based on Radio Propagation Modeling for Indoor WLANs. 2006 IEEE 63rd Vehicular Technology Conference, 2006, Vol. 6, pp. 2676–2680. doi:10.1109/VETECS.2006.1683354.
16. Shin, B.; Lee, J.H.; Lee, T.; Kim, H.S. Enhanced weighted K-nearest neighbor algorithm for indoor Wi-Fi positioning systems. 2012 8th International Conference on Computing Technology and Information Management (NCM and ICNIT), 2012, Vol. 2, pp. 574–577.

- 284 17. Husen, M.N.; Lee, S. Indoor Human Localization with Orientation Using WiFi Fingerprinting. Proceedings
285 of the 8th International Conference on Ubiquitous Information Management and Communication; ACM:
286 New York, NY, USA, 2014; ICUIMC '14, pp. 109:1–109:6. doi:10.1145/2557977.2557980.
- 287 18. Lin, T.; Fang, S.; Tseng, W.; Lee, C.; Hsieh, J. A Group-Discrimination-Based Access Point Selection
288 for WLAN Fingerprinting Localization. *IEEE Transactions on Vehicular Technology* **2014**, *63*, 3967–3976.
289 doi:10.1109/TVT.2014.2303141.
- 290 19. Chen, Z.; Zou, H.; Jiang, H.; Zhu, Q.; Soh, Y.; Xie, L. Fusion of WiFi, Smartphone Sensors and Landmarks
291 Using the Kalman Filter for Indoor Localization. *Sensors* **2015**, *15*, 715–732. doi:10.3390/s150100715.
- 292 20. Liu, H.; Darabi, H.; Banerjee, P.; Liu, J. Survey of Wireless Indoor Positioning Techniques and Systems.
293 *IEEE Transactions on Systems, Man and Cybernetics, Part C (Applications and Reviews)* **2007**, *37*, 1067–1080.
294 doi:10.1109/tsmcc.2007.905750.
- 295 21. Ma, R.; Guo, Q.; Hu, C.; Xue, J. An Improved WiFi Indoor Positioning Algorithm by Weighted Fusion.
296 *Sensors* **2015**, *15*, 21824–21843. doi:10.3390/s150921824.
- 297 22. Yiu, S.; Dashti, M.; Claussen, H.; Perez-Cruz, F. Locating user equipments and access points using RSSI
298 fingerprints: A Gaussian process approach. 2016 IEEE International Conference on Communications (ICC),
299 2016, pp. 1–6. doi:10.1109/ICC.2016.7511152.

300 © 2018 by the authors. Submitted to *Sensors* for possible open access publication under the terms and conditions
301 of the Creative Commons Attribution (CC BY) license (<http://creativecommons.org/licenses/by/4.0/>).